Cell Reports
Report

Networks of Polarized Actin Filaments in the Axon Initial Segment Provide a Mechanism for Sorting Axonal and Dendritic Proteins

Kaori Watanabe,[1] Sarmad Al-Bassam,[1] Yusuke Miyazaki,[2] Thomas J. Wandless,[2] Paul Webster,[3] and Don B. Arnold[1,*]
[1]Department of Biology, Program in Molecular and Computational Biology, University of Southern California, Los Angeles, CA 90089, USA
[2]Department of Chemical and Systems Biology, Stanford University, Stanford, CA 94305, USA
[3]Ahmanson Advanced EM and Imaging Center, House Research Institute, Los Angeles, CA 90057, USA
*Correspondence: darnold@usc.edu
http://dx.doi.org/10.1016/j.celrep.2012.11.015

SUMMARY

Trafficking of proteins specifically to the axonal or somatodendritic membrane allows neurons to establish and maintain polarized compartments with distinct morphology and function. Diverse evidence suggests that an actin-dependent vesicle filter within the axon initial segment (AIS) plays a critical role in polarized trafficking; however, no distinctive actin-based structures capable of comprising such a filter have been found within the AIS. Here, using correlative light and scanning electron microscopy, we visualized networks of actin filaments several microns wide within the AIS of cortical neurons in culture. Individual filaments within these patches are predominantly oriented with their plus ends facing toward the cell body, consistent with models of filter selectivity. Vesicles carrying dendritic proteins are much more likely to stop in regions occupied by the actin patches than in other regions, indicating that the patches likely prevent movement of dendritic proteins to the axon and thereby act as a vesicle filter.

INTRODUCTION

The establishment and maintenance of neuronal polarity is critically dependent on the correct targeting of newly synthesized proteins to the axonal and dendritic compartments. Yet, despite the central importance of polarized targeting for determining neuronal structure and function, it remains poorly understood. Transmembrane proteins are transported from the cell body to neuronal processes in transport vesicles pulled by kinesin motors along microtubules (Hirokawa, 1998); however, a variety of evidence suggests that kinesin motors do not autonomously direct vesicles to particular polarized compartments. Most axonal proteins are initially transported to both compartments, and later are concentrated on the membrane of the axon as a result of selective removal from the dendritic plasma membrane through endocytosis (Garrido et al., 2001; Sampo et al., 2003; Wisco et al., 2003). In contrast, vesicles that carry dendritic proteins, along with some of the kinesins that transport them, are found exclusively in the somatodendritic compartment (Burack et al., 2000; Setou et al., 2000). However, these kinesins cannot autonomously distinguish between axonal and dendritic microtubules, suggesting that other factors help to guide vesicles initially to the dendrites (Cai et al., 2009; Nakata and Hirokawa, 2003).

Recent work has suggested that actin and myosin motors play critical roles in the localization of neuronal proteins to polarized compartments. Interaction with Myosin Va is necessary and sufficient for localization of proteins to the somatodendritic compartment, and Myosin VI is similarly important for localization of proteins to the surface of the axon (Lewis et al., 2009, 2011). Live-imaging experiments have shown that vesicles carrying dendritic proteins enter both axons and dendrites with equal frequency. However, once they are inside the axon initial segment (AIS), almost all vesicles carrying dendritic proteins halt, and many reverse direction, in an actin- and Myosin-Va-dependent manner (Al-Bassam et al., 2012). In contrast, vesicles carrying axonal or nonspecifically localized proteins move efficiently through the AIS. These observations strongly suggest that a semipermeable, actin-dependent barrier within the AIS blocks the passage of vesicles carrying dendritic proteins, but allows passage of those carrying axonal or nonspecifically localized proteins.

Additional evidence points to the existence of a vesicle filter within the AIS. Transmembrane proteins are prevented from diffusing along the plasma membrane of the AIS between the cell body and the distal axon (Winckler et al., 1999). Similarly, large inert molecules are prevented from diffusing to the distal axon following injection into the cell body (Song et al., 2009). However, both transmembrane proteins and large cytoplasmic proteins move freely between the cell body and the distal axon in neurons treated with cytochalasin D or latrunculin A. Until now, no distinctive actin-based structures have been noted within the AIS in electron microscopy studies (Palay et al., 1968), and labeling neurons in culture with phalloidin according to standard protocols has revealed no specific labeling patterns within the AIS (Lewis et al., 2009). Here, we used correlative light and electron microscopy to image small networks of actin filaments arrayed in parallel within the AIS, a structure that is optimized to act as a semipermeable barrier. Vesicles carrying dendritic proteins are much more likely to stop at locations

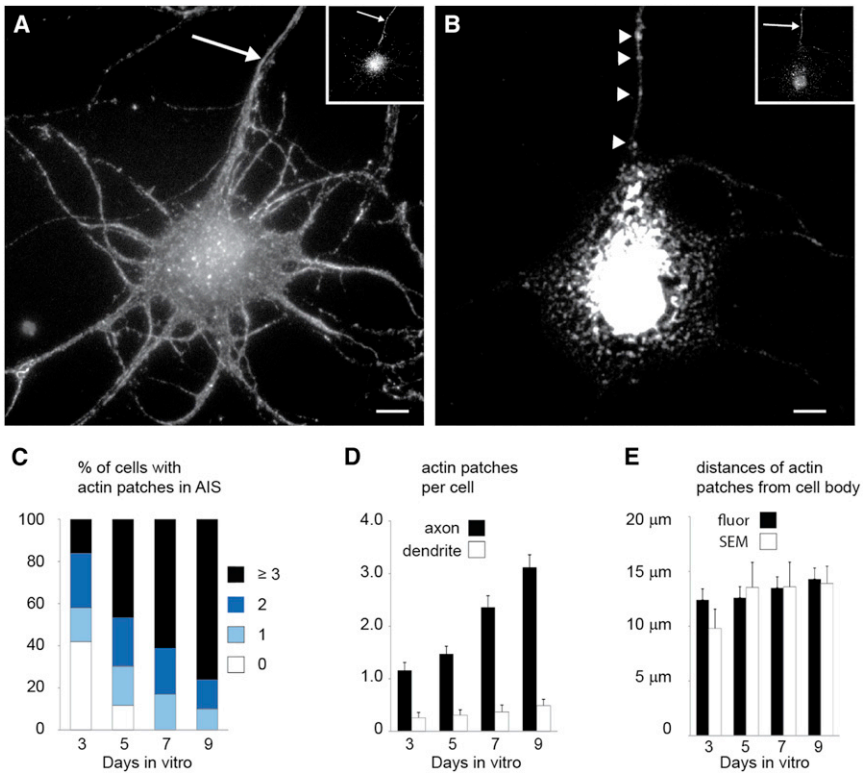

Figure 1. Actin within the AIS Is Concentrated in Patches

(A) Cortical neuron in dissociated culture stained with phalloidin following permeabilization with 0.1% TX-100 (see Extended Experimental Procedures) shows actin distributed diffusely throughout. Inset shows the same cell stained for Ankyrin G.

(B) A cell comparable to (A) permeabilized with 1% TX-100 shows actin in discrete patches in the axon (arrowheads). Inset shows the same cell stained for Ankyrin G.

(C) Percentages of cells with different numbers of actin patches at different times in vitro. By 7 DIV, 100% of cells have at least one actin patch.

(D) The number of actin patches per cell increases from one at 3 DIV to more than three at 9 DIV in the AIS (black bars), whereas actin patches are contained in fewer than one out of two dendrites (white bars).

(E) Analysis of fluorescence images (Fluor, black bars) and SEM images (white bars) indicates that most actin patches in the AIS are found between 10 μm and 15 μm away from the cell body.

Scale bars, 5 μm. The arrows points to the axon. Error bars represent SEM.

where actin networks are present, indicating that they behave like a vesicle filter.

RESULTS

Small Networks of Actin Filaments Are Found in the AIS

To look for actin-dependent structures within the AIS, we labeled cortical neurons in dissociated culture with phalloidin after permeabilizing them with 0.1% TX-100. Consistent with previous results, we found no unique labeling patterns within the AIS (Figure 1A). However, when the cortical neurons were subjected to slightly harsher permeabilization followed by phalloidin staining (1% TX-100), we found sharply delineated patches within the AIS (Figure 1B). Actin patches were found in 58% of cultured cortical neurons (n = 50 cells) at 3 days in vitro (DIV), and increased to 100% at 7 and 9 DIV (n = 41 and 50 cells, respectively; Figure 1C). Actin patches are up to six times more numerous in axons than in dendrites (Figure 1D), suggesting that their primary site of action is in the axon. Within the axon, they are found at an average distance of 13 ± 1 μm from the cell body (n = 184 cells), indicating that they are located predominantly within the AIS (Figure 1E).

To examine the fine structure of these patches, we used a whole-mount preparation similar to that described in Svitkina and Borisy (1998), which we imaged using scanning electron microscopy (SEM, Figure 2; see Experimental Procedures). Both axons, which were identified as the longest processes (Figure 2A), and dendrites contained longitudinally oriented fibers with a diameter of ~25 nm, indicating that they likely are microtubules (Figures 2B and 2D). Within the AIS there were also networks of small-diameter filaments (~10 nm in diameter) that were roughly the same size and at the same location as the actin patches stained with phalloidin (Figures 2B and 2C), but were found only rarely in dendrites (Figures 2D and 2E). To verify that these fibers were actin, as opposed to fibers of similar diameter, such as neurofilaments (Palay and Palade, 1955), we labeled cultures with heavy meromyosin (HMM), an actin-specific label (Pruyne et al., 2002). In HMM-labeled cultures of dissociated neurons (Figures 2F–2J) that were imaged by SEM, the labeled filaments were clearly identifiable by their frosted appearance (Figures 2I and 2J). In addition, the 10-nm-diameter fibers that were so prominent in the AIS of untreated neurons were not visible in HMM-labeled images (Figures 2B, 2I, and 2J), consistent with actin filaments being decorated with HMM. Actin in the HMM-labeled SEM images was arranged in discrete patches roughly 2–3 μm in diameter (Figure 2G; Figure S1), similar to its distribution in phalloidin-labeled fluorescence images (Figure 1B). In addition, the average distance from the cell body of actin patches measured on SEM images (13.2 ± 2 a.u., n = 75) was not significantly different from the same measurements on fluorescence images ($p > 0.5$, t test).

Actin Filaments Are Oriented with Their Plus Ends Facing Proximally

Because the results of experiments with Myosin Va and Myosin VI are consistent with actin filaments within the AIS being oriented with their plus ends facing toward the cell body (Arnold, 2009; Lewis et al., 2009, 2011), we directly tested whether actin within the AIS is oriented in a particular direction. To do so, we visualized the movements of myosin motors using a method

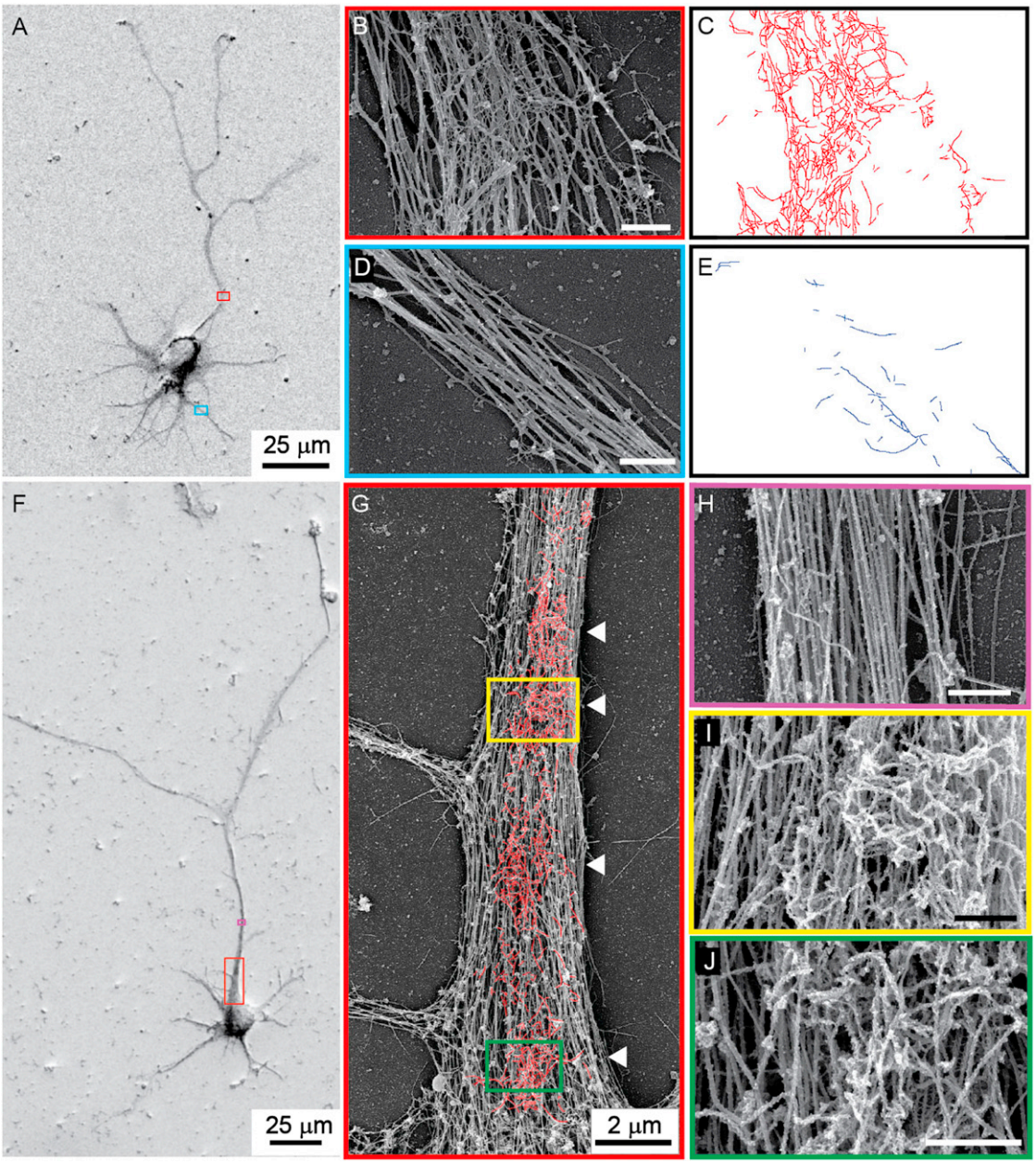

Figure 2. SEM Images of Actin Patches

(A) Cortical neuron in dissociated culture imaged by SEM. The long process with the overlapping red box is the axon.
(B) High-power view of the area bounded in red in (A). Two fiber types with diameters of 10 nm and 25 nm are visible.
(C) Outline of 10 nm fibers from (A).
(D) High-power view of area bounded in blue in (A), which contains a dendrite.
(E) Outline of 10 nm diameter fibers from (D) illustrates their relative paucity in dendrites compared with the axon (C).
(F) Cortical neuron in culture, coated with OsO_4 and platinum, labeled with HMM, and imaged by SEM.
(G) Medium-power image of the area in the red box in (F). HMM-labeled fibers are outlined in red. Arrowheads point to high-density actin patches.
(H) High-power image of the region in (F) bounded by purple and corresponding to the axon beyond the AIS. There is virtually no labeling by HMM.
(I and J) Regions bounded by yellow (I) and green (J) in (G) show actin filaments labeled with HMM that give a frosted appearance.
Scale bars, 500 nm unless otherwise indicated. See also Figure S1.

that was previously used to visualize movements of dynein (Kapitein et al., 2010a, 2010b). In particular, we examined the movements of Myosin Va, which moves in the plus direction toward the barbed ends of actin filaments (Krementsov et al., 2004), and of Myosin VI, which moves in the opposite direction toward the pointed end of actin filaments (Hasson and Mooseker, 1994).

By attaching an FKBP domain to a green fluorescent protein (GFP)-tagged transmembrane protein containing a peroxisome targeting signal (PEX-GFP-FKBP; Gould et al., 1989), and an FRB domain to a tailless myosin isoform (Myosin Va/VI-FRB), one can inducibly attach myosin to peroxisomes following the addition of iRap, a rapamycin analog (Inoue et al., 2005). The subsequent movements of the peroxisomes follow those of the motors to which they have been attached, allowing movements of the motors to be visualized. In addition, by comparing the changes in locations of peroxisomes before and after addition of iRap, one can map the locations and orientations of the fiber tracks along which the motor moves (Figure S2).

After PEX-GFP-FKBP and Myosin Va-FRB were expressed for 24–26 hr in dissociated cortical neurons, they did not colocalize; however, 1 hr after addition of iRap, the two proteins colocalized with high fidelity, indicating that Myosin Va interacted with the peroxisomes (Figure S2). In the absence of iRap 1.1% of peroxisomes moved >160 nm in 60 s (n = 174 peroxisomes), whereas in the presence of iRap, 19.3% of peroxisomes moved (n = 245 peroxisomes). Moreover, when iRAP was added in the presence of 2 μM Cytochalasin D, only 0.9% of peroxisomes moved (n = 110), indicating that actin filaments are necessary for peroxisome movements. The peroxisomes with Myosin Va-FRB that moved within the AIS showed a striking asymmetry in direction, with 80% of the movements directed toward the cell body (36 out of 45, n = 27 cells; Figures 3A and 3C; Figure S3). To further probe the orientation of actin filaments within the AIS, we created a fusion between FRB and Myosin VI (Myosin VI-FRB). When Myosin VI-FRB was expressed with PEX-GFP-FKBP in the presence of iRap, ~80% of nonstationary peroxisomes in the AIS moved away from the cell body (35 out of 44, n = 30 cells; Figures 3B and 3C). The results obtained with the two different motors are significantly different ($p < 0.0001$, Fisher's exact test), and each strongly suggests that the majority of actin filaments within the AIS are oriented with their plus ends facing the cell body. In contrast to the peroxisomes observed within the AIS, those within dendrites were equally likely to move distally as they were to move proximally, whether they interacted with Myosin Va (22 of 42 moved proximally, n = 27 cells; Figure 3C) or with Myosin VI (19 of 42 moved proximally, n = 30 cells; Figure 3C). The movements generated by Myosin Va and Myosin VI in dendrites were not significantly different from each other ($p > 0.5$, Fisher's exact test) but were significantly different from similar movements in the AIS ($p < 0.001$, Fisher's exact test). Thus, our results indicate that most actin filaments within the AIS are oriented in parallel with their plus ends facing the cell body, whereas actin filaments within the dendrites are equally likely to be oriented in either direction.

Measurements of peroxisome movement indicate that within the AIS these movements likely were mediated along actin filaments concentrated within patches (Figures 1 and 3). Overall, very few peroxisomes moved, consistent with movements occurring on actin in sparsely distributed patches. In addition, the locations of moving peroxisomes in the AIS attached to either Myosin Va or Myosin VI (12.4 ± 1 μm and 11.6 ± 1 μm from the cell body, respectively) were statistically indistinguishable from the locations of the actin patches measured from images of phalloidin immunostaining or SEM micrographs (Figure 1E; $p > 0.2$, t test). Furthermore, peroxisomes did not move more than 2 μm and had an average size of 0.7 μm, which is not statistically different from half the diameter of actin patches measured from SEM images ($p > 0.48$, t test; Figure 3D). Our results suggest that movements of myosin motors inducibly bound to peroxisomes occur on actin within patches. To test this hypothesis more specifically, we took cells in which vesicle movements

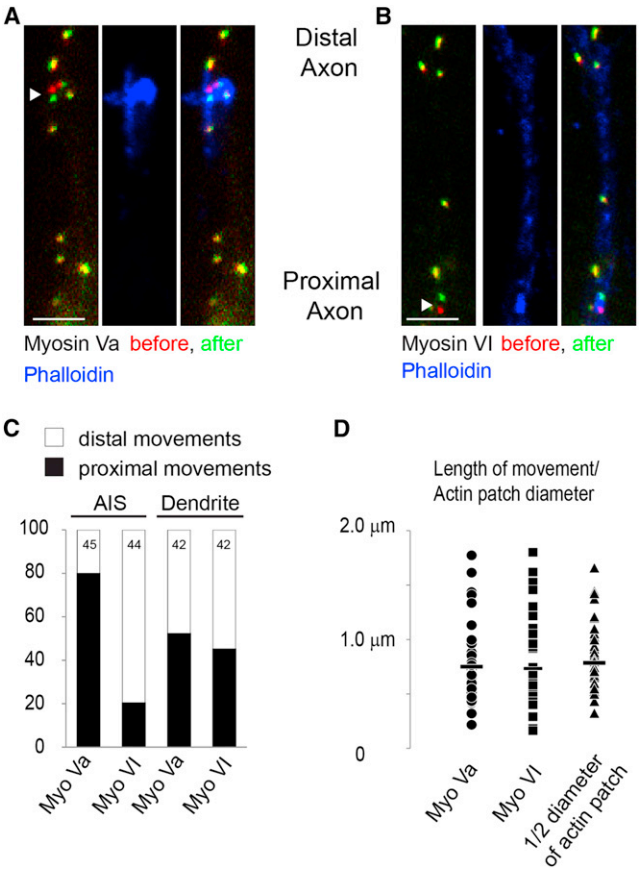

Figure 3. Mapping of Actin Filaments Using Peroxisome Movements Generated by Myosin Motors

(A) Peroxisomes labeled with GFP and bound to Myosin Va at time point 0 (red), and 60 s later (green). Most peroxisomes did not move and thus are colored in yellow. The arrowhead points to a peroxisome that moved toward the cell body. Note that the distal axon is at the top of the image and the proximal axon is oriented toward the bottom. Phalloidin staining in blue indicates that the peroxisome movement occurred at the same location as an actin patch. Scale bar, 2 μm.

(B) Similar to (A) except that peroxisomes are fastened to Myosin VI. Peroxisome indicated by the arrowhead moves toward the distal axon within an area characterized by high-density phalloidin staining corresponding to an actin patch. Scale bar, 2 μm.

(C) Approximately 80% of peroxisomes in the AIS attached to Myosin Va move toward the cell body, whereas ~80% of AIS peroxisomes attached to Myosin VI move distally. Roughly equal numbers of peroxisomes in dendrites move in both directions when attached to Myosin Va or Myosin VI.

(D) The lengths of peroxisome movements (mean indicated by bar) attached to Myosin Va (circle) or to Myosin VI (square) are comparable to half of the diameter of actin patches measured from SEM images (triangles).

See also Figures S2 and S3.

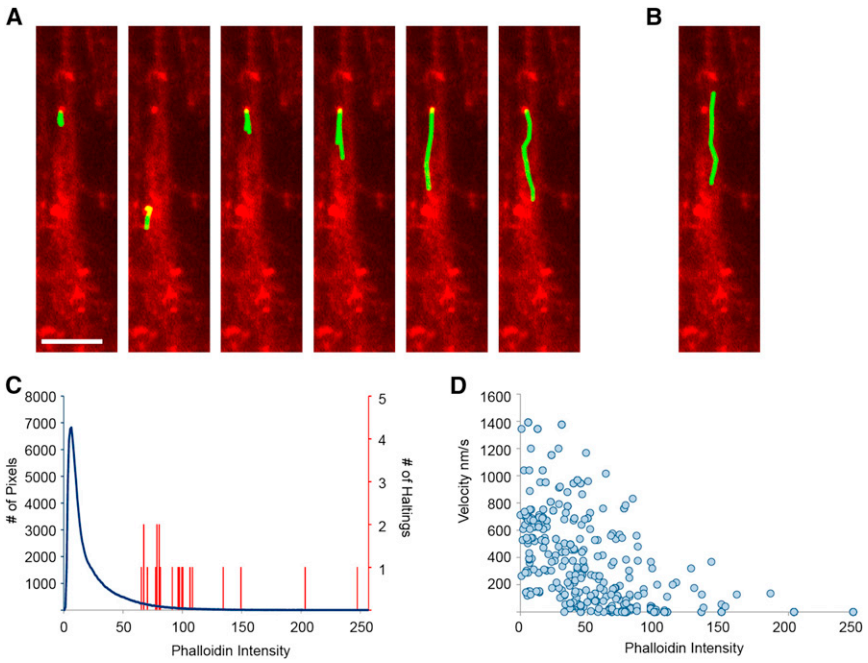

Figure 4. Vesicles Carrying a Dendritic Protein Tend to Halt in Regions with High Phalloidin

(A) Tracks (green) taken by vesicles carrying TfR-GFP-FM4 in the axon of a cortical neuron in dissociated culture. Phalloidin staining is shown in red. All vesicles originally travel in an upward direction, and all six stop in an area of concentrated phalloidin corresponding to an actin patch.

(B) The vesicle carrying TfR-GFP-FM4 that does not stop avoids areas of concentrated phalloidin staining.

(C) Histogram of phalloidin staining in individual pixels (blue) in the AIS (defined by expression of the AIS marker Nav1.2 II-III-HAmCherry; Al-Bassam et al., 2012) and of phalloidin staining in regions where vesicles halt for >5 s (red); 21 out of 21 locations where vesicles halted had levels of phalloidin staining in the top 6% of all pixels.

(D) Velocity versus phalloidin intensity for individual time points (taken every 1 s) shows an inverse relationship (n = 28 vesicles, 8 cells).

See also Figure S4 and Movie S1.

of peroxisomes had been observed, and then permeabilized and stained them with phalloidin so that actin patches could be visualized. We found that when images of actin patches were superimposed with images of peroxisome movement, the two overlapped (Figures 3A and 3B), indicating that the motors likely had been moving on actin within the patches. Together, these experiments demonstrate that the actin patches seen by epifluorescence microscopy and by SEM (Figures 1, 2, and 3) are not artifacts of preparation, but represent functional networks of parallel actin filaments.

Actin Networks Comprise a Vesicle Filter

Given that actin patches have properties that one would expect from components of a vesicle filter, we asked whether they might influence vesicle trafficking. To directly observe vesicles moving within the AIS following release from the Golgi, we expressed the transferrin receptor fused with GFP and with four tandem modified FKBP domains (TfR-GFP-FM4). After translation, this protein is sequestered within the endoplasmic reticulum and then released by addition of the FKBP ligand Shield-1 (Banaszynski et al., 2006). Previously, we found that vesicles carrying dendritic proteins freely entered the axon following release from the Golgi, but that once inside the AIS, almost all of them halted and some reversed direction before reaching the distal axon (Al-Bassam et al., 2012). To determine whether halting/reversing events occur in the same locations as actin patches, we first imaged vesicle movements in dissociated cortical neurons expressing TfR-GFP-FM4 after exposure to Shield-1, and then fixed, permeabilized, and stained the cells with phalloidin in order to image actin patches (Figure 1B). When we compared the movies of vesicles moving within the AIS with images of actin patches in the same neurons, we found a striking colocalization between locations where vesicles stopped/reversed and actin patches (Figures 4A and 4B; Figure S4; Movie S1). Furthermore, correlation of the locations where vesicles stopped with phalloidin staining showed that 21 out of the 21 vesicles (n = 8 cells) that stopped did so at locations where the magnitude of phalloidin staining was in the top 6% of all pixels within the AIS ($p < 0.0001$, binomial distribution; Figure 4C). In addition, the average amount of phalloidin at locations where the vesicles stopped (104 ± 10 a.u., n = 21 vesicles, 8 cells) was significantly higher than the average intensity of phalloidin in the AIS (21.6, $p < 0.001$, t test). This correlation between phalloidin staining and prevention of vesicle movement is further illustrated in a graph of vesicle velocity versus phalloidin intensity, which clearly shows the inverse relationship between the two variables (Figure 4D). Thus, it is clear that vesicles are overwhelmingly more likely to stop at locations with high concentrations of actin, that is, within actin patches. Thus, actin patches likely comprise the vesicle filter that prevents the movement of vesicles carrying dendritic proteins into the distal axon.

DISCUSSION

In this study, we have presented evidence of the presence of actin networks within the AIS that act as a semipermeable vesicle filter. Although staining with phalloidin under standard conditions showed no specific labeling of actin within the AIS, slightly harsher conditions revealed the presence of discrete patches of actin several microns in diameter in the AIS of 100% of cortical neurons following 7 days in culture. Imaging by SEM revealed that these patches contained dense networks of actin filaments that were labeled with the actin marker HMM. Furthermore, using a technique involving live imaging of myosin motors, we showed that roughly 80% of actin filaments are oriented with their plus ends facing the cell body. Such

a structure would prevent the passage of vesicles carrying plus-end-directed myosin motors, such as Myosin Va, while allowing passage of those associated with minus-end-directed myosins. Vesicles containing dendritic proteins in live cells halted almost exclusively at locations where actin patches were present, indicating that these actin networks act as a barrier to prevent vesicles carrying dendritic proteins from reaching the distal axon.

Networks of polarized actin filaments are also present in dendritic spines, where they are oriented such that their plus ends face the plasma membrane (Korobova and Svitkina, 2010). This orientation causes vesicles carrying dendritic proteins and associated with plus-end-directed myosins, such as Myosin Va, to be delivered to the plasma membrane (Correia et al., 2008), while those associated with Myosin VI travel toward the shaft of the dendrite (Osterweil et al., 2005). In contrast to dendritic spines, the actin networks within the AIS are oriented with their plus ends closest to the cell body. As a result of interaction with the two networks, vesicles associated with Myosin Va, such as those that transport GluR1 (Correia et al., 2008), avoid the axon, and once they are in the dendrites, they are directed toward the surface of spines. In contrast, vesicles that are associated with Myosin VI are transported out of the dendritic spines, and if they reach the AIS, they are preferentially transported toward the distal axon. Thus, vesicles associated with Myosin Va will deliver their contents to the dendritic spines, whereas those associated with Myosin VI will ultimately deliver theirs to the axon (Lewis et al., 2011).

A number of distinct structural elements distinguish the AIS from the axonal and somatodendritic compartments. Dense clusters of Na^+ and K^+ channels are present on the membrane of the AIS (Lorincz and Nusser, 2008; Wollner and Catterall, 1986), anchored by a complex structure consisting of Ankyrin G and β-Spectrin (Garrido et al., 2003; Komada and Soriano, 2002). Recent evidence showed that length of the AIS is variable and can affect the overall electrical excitability of the cell (Grubb and Burrone, 2010). Furthermore, the size of the AIS is determined by a boundary that is defined by Ankyrin B shortly after symmetry is broken (Galiano et al., 2012). Our work suggests that in addition to being the origin of action potentials, the AIS is also the location of critical vesicular trafficking events that determine the polarized structure of neurons. In the future, it will be important to determine whether the cytoskeletal scaffold that supports Na^+ and K^+ channels is physically connected to and functionally dependent on the actin networks described in this work.

By interacting with vesicles associated with either plus- or minus-end-directed myosins, the actin networks identified here can selectively target vesicles and their cargos to dendrites, allowing cells to establish and maintain polarized structure and function. However, it is not known how such filters arise. A clue as to how this might happen is found in experiments in which networks of parallel and antiparallel actin filaments were made to interact with myosin motors (Reymann et al., 2012). Remarkably, myosin motors caused the antiparallel filaments to depolymerize, whereas parallel filaments were left intact. Thus, interaction with myosin motors naturally leads to the development of polar networks such as those found in both the AIS and dendritic spines.

Another intriguing question concerns the time at which the polarized actin networks develop. As early as 3 DIV, actin patches are visible in >50% of neurons, suggesting that the actin network develops shortly after the breaking of symmetry in stage III neurons (Dotti et al., 1988). However, because actin patches are not present in 100% of neurons until 7 DIV, it would appear that the formation of actin networks occurs after events such as the activation of TGFβ (Yi et al., 2010) and the targeting of Kif5 isoforms to the nascent axon (Jacobson et al., 2006), which is thought to be mediated by the concentration of GTP-tubulin in such processes (Nakata et al., 2011). In the future, it will be important to determine whether the establishment of actin networks is directly connected to these events and, if so, by what mechanism.

In conclusion, we have presented evidence that patches of actin filaments oriented with their plus ends facing toward the cell body are located within the AIS. Although actin filaments were previously shown to form networks of fibers with a predominant orientation within dendritic spines (Korobova and Svitkina, 2010) and growth cones (Lewis and Bridgman, 1992), our results demonstrate that such networks exist within the AIS. Furthermore, our results suggest that these actin patches can constitute a vesicle filter that, in combination with myosin motors, prevents vesicles carrying dendritic proteins from entering the distal axon.

EXPERIMENTAL PROCEDURES

Cell Membrane Extraction and SEM Processing

Cell membranes were extracted with M buffer (50 mM imidazole [pH 6.9], 0.5 mM $MgCl_2$, 500 mM KCl, 1 mM EGTA, 0.1 mM EDTA) containing 1% Triton X-100, 4% polyethylene glycol (molecular weight = 8 kDa) and 5 μM phalloidin for 8–15 min at room temperature. Cells were then washed with M buffer with 0.5 μM phalloidin four times and incubated with 0.25 mg/ml of HMM in M buffer (for HMM-coated cells) or M buffer (for non-HMM-coated cells) with 0.5 μM phalloidin for 30 min at room temperature. The cells were washed with water five times and fixed in 1% glutaraldehyde in 50 mM phosphate buffer (pH 6.9) and 2% tannic acid. The cells were then incubated in 1% OsO_4 for 1 hr, thiocarbohydrizide for 2 hr, and again in 1% OsO_4 for 1 hr at room temperature. The cells were dehydrated in EtOH, critical point dried, and coated with 3–7 nm platinum. This method was modified from one originally published by Svitkina and Borisy (1998).

Phalloidin Staining

Cell membranes were extracted by incubating cells with PBS containing Triton X-100 (1% for DIV 3–9 and 2% for DIV 12–16) and 1 μM phalloidin-Alexa-647 (or Alexa-594) for 8–15 min at room temperature. Cells were then fixed in 4% paraformaldehyde for 5 min at room temperature and left for immunocytochemistry.

Cell Transfection

Rat cortical neurons were prepared as described previously (Lewis et al., 2009). Experimental protocols were conducted according to the U.S. National Institutes of Health guidelines for animal research and were approved by the Institutional Animal Care and Use Committee at the University of Southern California.

Immunocytochemistry

Details regarding immunocytochemistry are described in Lewis et al. (2009). The primary antibodies used were chicken anti-GFP (Aves) 1:1,000, mouse anti-hemagglutinin (anti-HA; Covance) 1:500, and rabbit anti-Ankyrin G (Santa Cruz) 1:1,000. Secondary antibodies were conjugated to Alexa 488, 594, and 647 fluorophores (Invitrogen).

Analysis of FKBP-Myosin Experiments

Peroxisome movement was determined by overlapping of images taken at intervals of 60 s (ImageJ, NIH, Wayne Rasband; Mosaic plugin, ETH). Peroxisomes were determined to have moved when their positions (as determined by the center of mass calculated from the distribution of fluorescence associated with each peroxisome) changed by at least 160 nm. Only proximal or distal movements were recorded. An image of Nav1.2 II-III-HAmCherry was taken concurrently with the second image, and immediately afterward the cells were fixed for subsequent immunostaining. Actin filaments were stained with phalloidin, and the AIS marker Nav1.2 II-III-HAmCherry was stained using an anti-HA antibody. The live image was then aligned with the fixed image by matching the live and fixed Nav1.2 II-III-HAmCherry images. All analysis was done by blinded observers.

Analysis of TfR Vesicle Experiments

Details of the processing and tracking movies are described elsewhere (Al-Bassam et al., 2012). Immediately following imaging of vesicles containing TfR-GFP-FM4, cells were fixed and subsequently immunostained for phalloidin and GFP. Live images of TfR-GFP-FM4, which show the outline of the cell, were compared with anti-GFP images from fixed, immunostained cells, allowing the images of live and fixed neurons to be aligned. Vesicles were considered to have stopped when they moved 2 pixels (160 nm) or less for a time period longer than 5 s. The fluorescence intensity of phalloidin staining was normalized to 256 levels for each image. The fluorescence intensity in the area where a vesicle stopped was determined by taking the average fluorescence intensity in a 3×3 grid surrounding the vesicle. The instantaneous velocity of each vesicle was calculated by distance moved divided by the time between each successive frame using the MTrackJ plugin (Eric Meijering).

Measurement of Distance from the Cell Body

The distance from the cell body was measured from a line drawn between the two points where the axon met the cell body. Distances were measured from this point to the starting point of a moving peroxisome, the center of phalloidin staining, or the center of actin filaments.

Measurement of Actin Patches

The diameter of actin patches was obtained by taking the average of the distance parallel to the axon and the distance perpendicular to the axon.

For additional details, please see the Extended Experimental Procedures.

SUPPLEMENTAL INFORMATION

Supplemental Information includes Extended Experimental Procedures and four figures and can be found with this article online at http://dx.doi.org/10.1016/j.celrep.2012.11.015.

LICENSING INFORMATION

ACKNOWLEDGMENTS

The authors thank Samantha Ancona for help in data analysis, and Emily Liman for helpful discussions. This work was supported by NIH grants NS041963 and MH086381 to D.B.A., and GM073046 to T.J.W.

Received: September 26, 2012
Revised: November 10, 2012
Accepted: November 21, 2012
Published: December 13, 2012

REFERENCES

Al-Bassam, S., Xu, M., Wandless, T.J., and Arnold, D.B. (2012). Differential trafficking of transport vesicles contributes to the localization of dendritic proteins. Cell Rep. *2*, 89–100.

Arnold, D.B. (2009). Actin and microtubule-based cytoskeletal cues direct polarized targeting of proteins in neurons. Sci. Signal. *2*, pe49.

Banaszynski, L.A., Chen, L.C., Maynard-Smith, L.A., Ooi, A.G., and Wandless, T.J. (2006). A rapid, reversible, and tunable method to regulate protein function in living cells using synthetic small molecules. Cell *126*, 995–1004.

Burack, M.A., Silverman, M.A., and Banker, G. (2000). The role of selective transport in neuronal protein sorting. Neuron *26*, 465–472.

Cai, D., McEwen, D.P., Martens, J.R., Meyhofer, E., and Verhey, K.J. (2009). Single molecule imaging reveals differences in microtubule track selection between Kinesin motors. PLoS Biol. *7*, e1000216.

Correia, S.S., Bassani, S., Brown, T.C., Lisé, M.F., Backos, D.S., El-Husseini, A., Passafaro, M., and Esteban, J.A. (2008). Motor protein-dependent transport of AMPA receptors into spines during long-term potentiation. Nat. Neurosci. *11*, 457–466.

Dotti, C.G., Sullivan, C.A., and Banker, G.A. (1988). The establishment of polarity by hippocampal neurons in culture. J. Neurosci. *8*, 1454–1468.

Galiano, M.R., Jha, S., Ho, T.S., Zhang, C., Ogawa, Y., Chang, K.J., Stankewich, M.C., Mohler, P.J., and Rasband, M.N. (2012). A distal axonal cytoskeleton forms an intra-axonal boundary that controls axon initial segment assembly. Cell *149*, 1125–1139.

Garrido, J.J., Fernandes, F., Giraud, P., Mouret, I., Pasqualini, E., Fache, M.P., Jullien, F., and Dargent, B. (2001). Identification of an axonal determinant in the C-terminus of the sodium channel Na(v)1.2. EMBO J. *20*, 5950–5961.

Garrido, J.J., Giraud, P., Carlier, E., Fernandes, F., Moussif, A., Fache, M.P., Debanne, D., and Dargent, B. (2003). A targeting motif involved in sodium channel clustering at the axonal initial segment. Science *300*, 2091–2094.

Gould, S.J., Keller, G.A., Hosken, N., Wilkinson, J., and Subramani, S. (1989). A conserved tripeptide sorts proteins to peroxisomes. J. Cell Biol. *108*, 1657–1664.

Grubb, M.S., and Burrone, J. (2010). Activity-dependent relocation of the axon initial segment fine-tunes neuronal excitability. Nature *465*, 1070–1074.

Hasson, T., and Mooseker, M.S. (1994). Porcine myosin-VI: characterization of a new mammalian unconventional myosin. J. Cell Biol. *127*, 425–440.

Hirokawa, N. (1998). Kinesin and dynein superfamily proteins and the mechanism of organelle transport. Science *279*, 519–526.

Inoue, T., Heo, W.D., Grimley, J.S., Wandless, T.J., and Meyer, T. (2005). An inducible translocation strategy to rapidly activate and inhibit small GTPase signaling pathways. Nat. Methods *2*, 415–418.

Jacobson, C., Schnapp, B., and Banker, G.A. (2006). A change in the selective translocation of the Kinesin-1 motor domain marks the initial specification of the axon. Neuron *49*, 797–804.

Kapitein, L.C., Schlager, M.A., Kuijpers, M., Wulf, P.S., van Spronsen, M., MacKintosh, F.C., and Hoogenraad, C.C. (2010a). Mixed microtubules steer dynein-driven cargo transport into dendrites. Curr. Biol. *20*, 290–299.

Kapitein, L.C., Schlager, M.A., van der Zwan, W.A., Wulf, P.S., Keijzer, N., and Hoogenraad, C.C. (2010b). Probing intracellular motor protein activity using an inducible cargo trafficking assay. Biophys. J. *99*, 2143–2152.

Komada, M., and Soriano, P. (2002). [Beta]IV-spectrin regulates sodium channel clustering through ankyrin-G at axon initial segments and nodes of Ranvier. J. Cell Biol. *156*, 337–348.

Korobova, F., and Svitkina, T. (2010). Molecular architecture of synaptic actin cytoskeleton in hippocampal neurons reveals a mechanism of dendritic spine morphogenesis. Mol. Biol. Cell *21*, 165–176.

Krementsov, D.N., Krementsova, E.B., and Trybus, K.M. (2004). Myosin V: regulation by calcium, calmodulin, and the tail domain. J. Cell Biol. *164*, 877–886.

Lewis, A.K., and Bridgman, P.C. (1992). Nerve growth cone lamellipodia contain two populations of actin filaments that differ in organization and polarity. J. Cell Biol. *119*, 1219–1243.

Lewis, T.L., Jr., Mao, T., Svoboda, K., and Arnold, D.B. (2009). Myosin-dependent targeting of transmembrane proteins to neuronal dendrites. Nat. Neurosci. *12*, 568–576.

Lewis, T.L., Jr., Mao, T., and Arnold, D.B. (2011). A role for myosin VI in the localization of axonal proteins. PLoS Biol. *9*, e1001021.

Lorincz, A., and Nusser, Z. (2008). Cell-type-dependent molecular composition of the axon initial segment. J. Neurosci. *28*, 14329–14340.

Nakata, T., and Hirokawa, N. (2003). Microtubules provide directional cues for polarized axonal transport through interaction with kinesin motor head. J. Cell Biol. *162*, 1045–1055.

Nakata, T., Niwa, S., Okada, Y., Perez, F., and Hirokawa, N. (2011). Preferential binding of a kinesin-1 motor to GTP-tubulin-rich microtubules underlies polarized vesicle transport. J. Cell Biol. *194*, 245–255.

Osterweil, E., Wells, D.G., and Mooseker, M.S. (2005). A role for myosin VI in postsynaptic structure and glutamate receptor endocytosis. J. Cell Biol. *168*, 329–338.

Palay, S.L., and Palade, G.E. (1955). The fine structure of neurons. J. Biophys. Biochem. Cytol. *1*, 69–88.

Palay, S.L., Sotelo, C., Peters, A., and Orkand, P.M. (1968). The axon hillock and the initial segment. J. Cell Biol. *38*, 193–201.

Pruyne, D., Evangelista, M., Yang, C., Bi, E., Zigmond, S., Bretscher, A., and Boone, C. (2002). Role of formins in actin assembly: nucleation and barbed-end association. Science *297*, 612–615.

Reymann, A.C., Boujemaa-Paterski, R., Martiel, J.L., Guérin, C., Cao, W., Chin, H.F., De La Cruz, E.M., Théry, M., and Blanchoin, L. (2012). Actin network architecture can determine myosin motor activity. Science *336*, 1310–1314.

Sampo, B., Kaech, S., Kunz, S., and Banker, G. (2003). Two distinct mechanisms target membrane proteins to the axonal surface. Neuron *37*, 611–624.

Setou, M., Nakagawa, T., Seog, D.H., and Hirokawa, N. (2000). Kinesin superfamily motor protein KIF17 and mLin-10 in NMDA receptor-containing vesicle transport. Science *288*, 1796–1802.

Song, A.H., Wang, D., Chen, G., Li, Y., Luo, J., Duan, S., and Poo, M.M. (2009). A selective filter for cytoplasmic transport at the axon initial segment. Cell *136*, 1148–1160.

Svitkina, T.M., and Borisy, G.G. (1998). Correlative light and electron microscopy of the cytoskeleton of cultured cells. Methods Enzymol. *298*, 570–592.

Winckler, B., Forscher, P., and Mellman, I. (1999). A diffusion barrier maintains distribution of membrane proteins in polarized neurons. Nature *397*, 698–701.

Wisco, D., Anderson, E.D., Chang, M.C., Norden, C., Boiko, T., Fölsch, H., and Winckler, B. (2003). Uncovering multiple axonal targeting pathways in hippocampal neurons. J. Cell Biol. *162*, 1317–1328.

Wollner, D.A., and Catterall, W.A. (1986). Localization of sodium channels in axon hillocks and initial segments of retinal ganglion cells. Proc. Natl. Acad. Sci. USA *83*, 8424–8428.

Yi, J.J., Barnes, A.P., Hand, R., Polleux, F., and Ehlers, M.D. (2010). TGF-beta signaling specifies axons during brain development. Cell *142*, 144–157.